Journal of
Materials Chemistry C

Accepted Manuscript

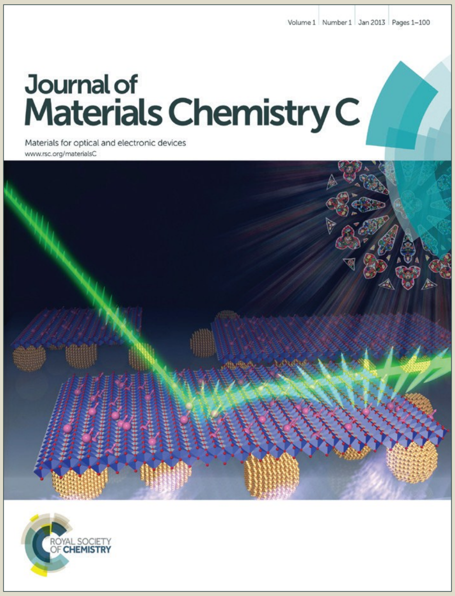

ROYAL SOCIETY
OF **CHEMISTRY**

www.rsc.org/materialsC

Journal Name

ARTICLE

Excimer Emission Based on Control of Molecular Structure and Intermolecular Interactions

Received 00th January 20xx,
Accepted 00th January 20xx

DOI: 10.1039/x0xx00000x

www.rsc.org/

Jaehyun Lee[a], Hyocheol Jung[a], Hwangyu Shin[a], Joonghan Kim[a], Daisuke Yokoyama[b], Hidetaka Nishimura[c], Atsushi Wakamiya[c], and Jongwook Park*[a]

Three triple-core chromophore derivatives based on anthracene and pyrene or chrysene moieties, 1,6-bis-(10-[1,1';3',1'']terphenyl-5'-yl-anthracen-9-yl)-pyrene (1,6 DAP-TP), 6,12-bis-(10-[1,1';3',1'']terphenyl-5'-yl-anthracen-9-yl)-chrysene (DAC-TP), and 2,7-bis-(10-[1,1';3',1'']terphenyl-5'-yl-anthracen-9-yl)-pyrene (2,7 DAP-TP), were designed and synthesized. For 1,6 DAP-TP, anthracene was attached to the 1,6 positions of pyrene. In the case of DAC-TP, two anthracenes were connected to chrysene, located at the center position within the core, whereas in 2,7 DAP-TP anthracene was connected to the 2, 7 positions of pyrene. All three materials had highly twisted core structures and bulky m-terphenyl side groups introduced in the core. Excimer emission was observed in the solid film state and can be interpreted as the result of anisotropic intermolecular alignment (orientation effect). The wavelength of excimer formation was controlled through the change of the center position of the triple-core chromophore, and the color coordinate of white light and efficiency could be controlled when the materials were used in an electroluminescence (EL) device. Excimer EL emissions of 1,6 DAP-TP, DAC-TP, and 2,7 DAP-TP were at 591 nm, 556 nm, and 538 nm, respectively, and CIE coordinate values of the devices were (0.37, 0.31), (0.30, 0.37), and (0.32, 0.44), respectively, showing single molecular white emission. 2,7 DAP-TP, showed a white OLED efficiency of 6.01 cd/A at 10 mA/cm^2.

Introduction

π-Conjugated compounds are useful in a variety of applications, including organic light-emitting diodes (OLEDs)[1], organic thin film transistors (OTFTs)[2], and organic photovoltaic cells (OPVCs)[3]. Two key determinants of the performance of such compounds in these applications are molecular structure and molecular interactions.[4] Thus, the molecular interactions of π-conjugated compounds have been widely studied.

To understand the relationship between molecular structure and interaction, research on intermolecular interactions[5], intramolecular interactions[6], charge transfer[7], and theoretical models of interacting molecules[8] have been performed. Excimers are dimeric species that are associated in an excited electronic state but dissociated in their ground electronic state. Since their first report[9], excimers have been intensively researched and the mechanism of aggregation has been elucidated.[10] Excimer formation is favored by a rigid, planar molecular structure, such as is found in anthracene[11], pyrene[12], and fluorene[13]. These representative chemical structures can form an aggregated state through large π-π overlap. Also, it is generally accepted that, if the molecular structure includes highly twisted and bulky substituents, aggregate formation is suppressed by steric hindrance.[14]

Excimer emission has the characteristic of showing a bathochromic shifted fluorescence spectrum resulting from the interaction between molecules in close contact. The magnitude of this wavelength change depends on the molecular interactions and molecular packing structure.[15] Thus, when developing π-conjugated compounds for use in applications such as OLEDs, OTFTs, and OPVCs, the ability to control the molecular packing structure during film deposition so as to optimize excimer formation is of great importance.[16]

Excimer formation of various derivatives is being researched for application in areas such as detection of DNA or guest molecules and sensing environmental parameters.[17] Also, excimer emission typically shows a broad absorption feature with a large full width at half maximum (FWHM). This characteristic can provide an advantage in white lighting applications, in order to obtain a high color rendering index in OLEDs.[18]

We recently reported a chromophore material, 1,6-bis-(10-[1,1';3',1'']terphenyl-5'-yl-anthracen-9-yl)-pyrene (1,6 DAP-TP), containing anthracene and pyrene that exhibit single molecular white emission, as well as controlled excimer emission.[19] Although a bulky side group is introduced into the highly twisted core group, molecular orientation is controlled

---

[a] *Department of Chemistry/Display Research Center, The Catholic University of Korea, Bucheon, 420-743, South Korea. Fax: +82-2-2164-4764; Tel: +82-2-2164-4821; *E-mail: hahapark@catholic.ac.kr*
[b] *Department of Organic Device Engineering and Research Center for Organic Electronics (ROEL), Yamagata University, 4-3-16, Johnan, Yonezawa, Yamagata, 992-8510, Japan*
[c] *Institute for Chemical Research, Kyoto University, Uji, Kyoto, 611-0011, Japan*

† Footnotes relating to the title and/or authors should appear here.

Electronic Supplementary Information (ESI) available: See DOI: 10.1039/x0xx00000x

and excimer formation and excimer emission are observed in the photoluminescence (PL) and electroluminescence (EL) spectra for 1,6 DAP-TP. A white OLED (WOLED) device was obtained with Commission Internationale de l'Eclairage (CIE) coordinates of (0.37, 0.31), a sharp FWHM value of 68 nm, and luminance efficiency of 3.43 cd/A.

In this study, triple-core chromophore derivatives were introduced to control the wavelengths of excimer emission to study the effects on WOLEDs devices (see Scheme 1). Triple-core chromophore derivatives connect a single molecule to three core chromophores. In 1,6 DAP-TP, anthracene is attached to the 1,6 positions of pyrene. In 6,12-bis-(10-[1,1';3',1'']terphenyl-5'-yl-anthracen-9-yl)-chrysene (DAC-TP), the triple core form has two anthracenes and a chrysene at the center. In contrast to 1,6 DAP-TP, in 2,7-bis-(10-[1,1';3',1'']terphenyl-5'-yl-anthracen-9-yl)-pyrene (2,7 DAP-TP) anthracenes are attached at the 2,7 positions of pyrene. The core chromophores each have a highly twisted structure and are connected orthogonally to each other. In addition, bulky m-terphenyl side groups are attached to the triple core of each molecule. The different triple-core chromophores examined in this work were designed to systematically modify the EL device and physical properties, along with the excimer emission wavelengths caused by derivatives.

Results and discussion

Scheme 1 shows the chemical structures of the synthesized compounds. 1,6 DAP-TP and 2,7 DAP-TP are triple core structures of anthracene-pyrene-anthracene, and DAC-TP is a triple-core chromophore of anthracene-chrysene-anthracene. m-Terphenyl groups were included as bulky side groups. All compounds were purified by recrystallization and column chromatography. The synthesized compounds were characterized using nuclear magnetic resonance (NMR) spectroscopy, mass spectroscopy and elemental analysis. The synthetic method for 1,6 DAP-TP was described in ref. 19. The synthetic methods for DAC-TP and 2,7 DAP-TP are shown in Scheme 2. Boronylation, bromination, and Suzuki aryl-aryl coupling reactions were used in the synthesis. The synthetic methods are described in more detail in the Experimental section.

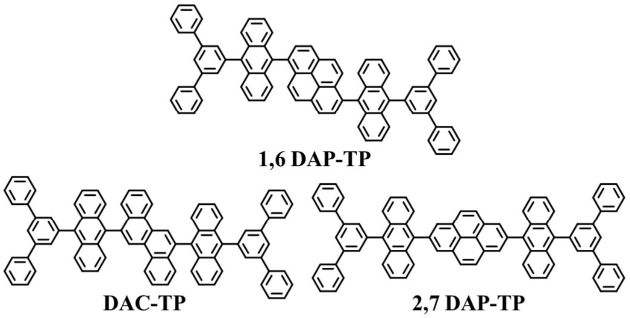

Scheme 1 Chemical structures of the triple-core chromophore derivatives.

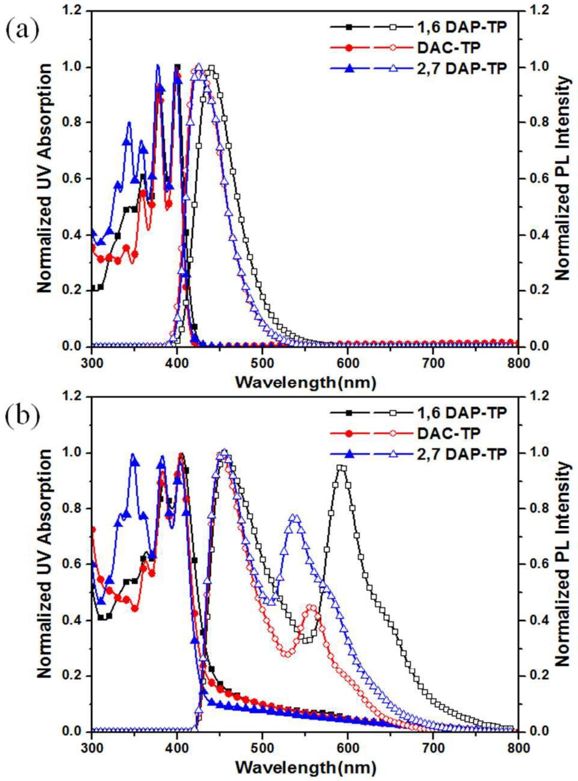

Fig. 1 UV-vis. absorption spectra and PL spectra of the synthesized materials: (a) 1 × 10^{-5} M THF solution, (b) vacuum-deposited film (filled symbols: UV-vis. absorption spectra, open symbols: PL spectra).

Table 1. Physical properties of 1,6 DAP-TP, DAC-TP, and 2,7 DAP-TP

Compounds	λ_{max} abs (nm) solns [a]/films [b]		λ_{max} PL (nm) solns [a]/films [b]		HOMO (eV) [e]	LUMO (eV) [f]	Band gap (eV)	T_g (°C)	T_d (°C)
1,6 DAP-TP	359, 379, 400	364, 384, 405	439	455, 591	-5.76	-2.88	2.88	220	511
DAC-TP	359, 378, 399	363, 382, 404	424	453, 556	-5.80	-2.85	2.95	191	574
2,7 DAP-TP	358, 377, 398	361, 382, 404	424	454, 537	-5.76	-2.82	2.94	204	516

[a] Measured in THF solution (1 x 10^{-5}M). [b] Measured in neat films (thickness: 50 nm). [c] Ultraviolet photoelectron spectroscopy (Riken-Keiki, AC-2). [d] LUMO obtained from the HOMO and the optical band gap.

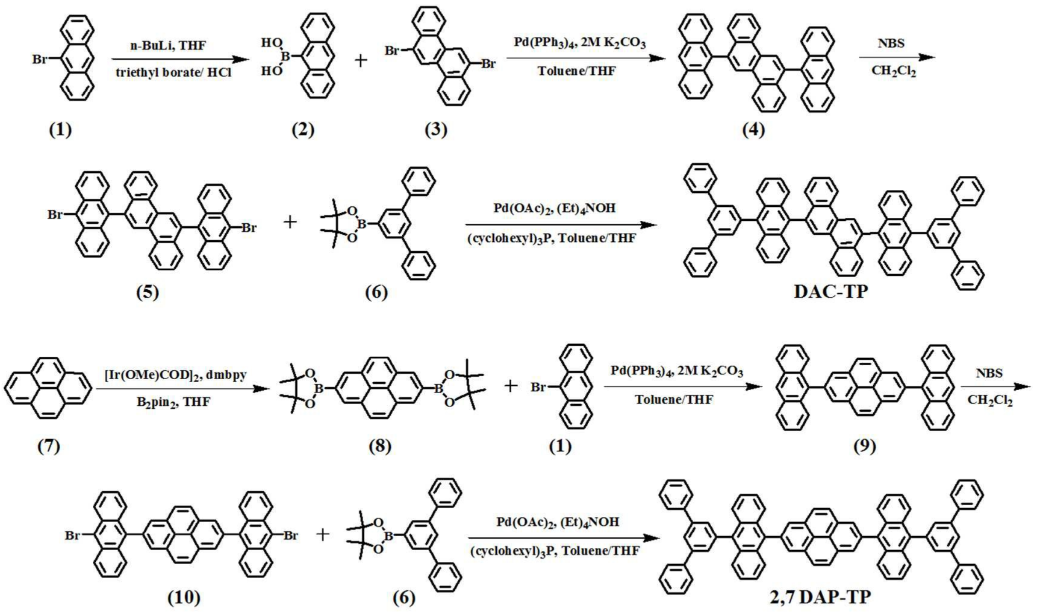

Scheme. 2 Synthetic routes for DAC-TP and 2,7 DAP-TP.

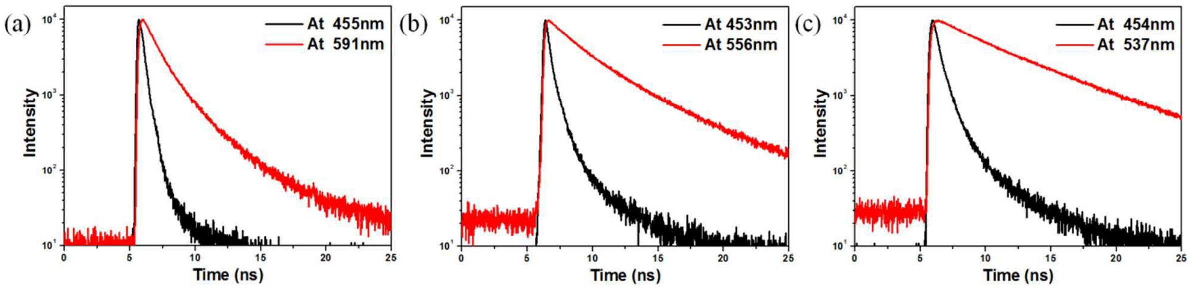

Fig. 2 Time-resolved emission decays obtained from the vacuum-deposited films (thickness: 50 nm) of (a) 1,6 DAP-TP, (b) DAC-TP, and (c) 2,7 DAP-TP.

UV-visible (UV-vis.) absorption and PL spectra of 1,6 DAP-TP, DAC-TP, and 2,7 DAP-TP are shown in Fig. 1. Spectra were collected in solution (1×10^{-5} M in THF) and solid state (vacuum-deposited 50 nm thick film). Optical properties are summarized in Table 1. Absorption maximum peak wavelengths ranged from 350 nm to 400 nm, which is typical of anthracene. For all three materials, the PL spectra in solution showed a maximum in the blue region in the range of 424 nm to 439 nm. In the vacuum-deposited film, the PL of 1,6 DAP-TP showed blue region emission at 455 nm and also showed excimer emission in the orange region at 591 nm. For DAC-TP, blue peak emission occurred at 453 nm, similar to 1,6 DAP-TP. On the other hand, an additional peak was observed in the yellow-green area of 556 nm. For 2,7 DAP-TP, PL peaks at 454 nm (blue emission) and 537 nm (green emission) were observed.

Unlike the solution state, which showed a single peak corresponding to PL emission from the molecule, the film samples exhibited emission peaks corresponding to molecular emission and excimer emission produced by molecular interactions. To examine the excimer emission behavior, time-resolved fluorescence spectroscopy of the three materials prepared as films was performed to obtain the decay time of the emission peak in the blue, green, yellow-green, and orange emission regions (see Fig. 2). For 1,6 DAP-TP, the average lifetimes (τ_{avg}) of the 455 and 591 nm emission peaks were 0.24 ns and 1.30 ns, respectively. The τ_{avg} for DAC-TP was 0.32 ns for the 453 nm peak and 3.15 ns for the 556 nm peak. For 2,7 DAP-TP, τ_{avg} was 0.35 ns for the 454 nm peak and 5.28 ns for the 537 nm peak (see Table S1). The longer PL lifetime in the green to orange region can be attributed to excimer formation.[20] To confirm this region was indeed excimer emission, the change in emission spectrum was observed as the temperature was increased (see Fig. S4(a)). Excimer emission intensity increases with an increase in temperature, as molecular motion becomes activated.[21] The PL emission intensity change of 2,7 DAP-TP film was measured under conditions of increasing temperature. At low temperatures (30°C), blue emission was dominant in the PL spectrum. An increase in emission intensity near 540 nm was observed with

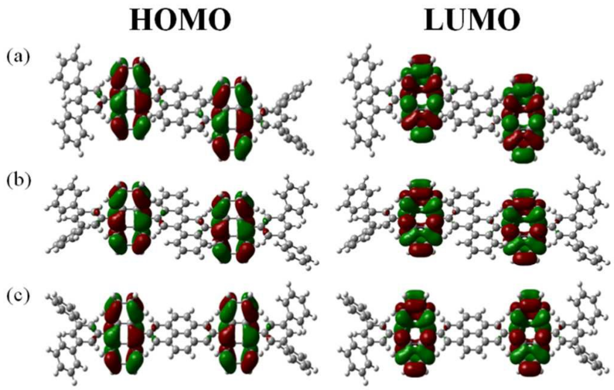

Fig. 3 HOMO and LUMO shapes of (a) 1,6 DAP-TP, (b) DAC-TP, (c) 2,7 DAP-TP (calculated at the B3LYP / 6-31G (d) level of theory).

increasing temperature, indicating increased formation of aggregates (stacks) at higher temperatures. To examine the effect of concentration on excimer formation, PL emission by 2,7 DAP-TP was measured at various concentrations (Fig. S4(b)). When the concentration was increased from 1 x 10^{-3} M to 1 x 10^{-2} M, the excimer emission intensity increased. This increase in intensity can be attributed to a decrease in intermolecular distance as the concentration increases.[10a]

The highest occupied molecular orbital (HOMO) and lowest unoccupied molecular orbital (LUMO) of the three compounds are shown in Fig. 3. The electron density was found to be distributed across the anthracene group, indicating that electron transfer between the ground state and the excited state could only occur within the anthracene moiety. Thus, efforts to tune the UV-vis. and PL spectra should concentrate on varying the anthracene group properties. The excimer emissions in the PL spectrum are expected to arise from intermolecular interactions of the anthracene planes. The HOMO and LUMO levels of the three materials showed similar values in the range of -5.76 to -5.80 eV and -2.88 to -2.82 eV, respectively.

The glass transition temperatures (T_g) and the decomposition temperatures (T_d) of the compounds were determined with differential scanning calorimetry (DSC) and thermogravimetric analysis (TGA), respectively (Table 1). The T_g values of 1,6 DAP-TP, DAC-TP and 2,7 DAP-TP were 220 °C, 191 °C and 204 °C, respectively, while the T_d values were 511 °C, 574 °C, and 516 °C, respectively. These findings showed that all three materials had excellent thermal properties.

To check the molecular orientation within the film, variable angle spectroscopic ellipsometry (VASE) analysis was performed.[16, 22] Fig. 4 shows the anisotropies in refractive index and extinction coefficient as a function of wavelength. For 1,6 DAP-TP and 2,7 DAP-TP, extinction coefficient values (dotted line) of the vertical component were much smaller than those of the horizontal component (solid line). This indicates that the two compounds orient with a significant dipole in the horizontal direction. This trend towards horizontal alignment can be explained by the linear molecular structure, and would be expected to promote excimer formation.[19] However for DAC-TP, VASE analysis was difficult and the related information could not be obtained.

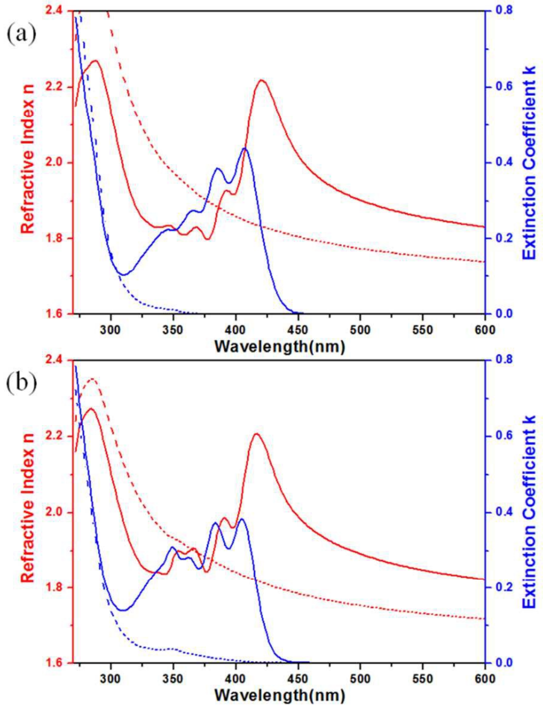

Fig. 4 Optical anisotropy of the films prepared from the (a) 1,6 DAP-TP, (b) 2,7 DAP-TP: anisotropic refractive indices n and extinction coefficients k. The solid lines (n_o and k_o) and dotted lines (n_e and k_e) indicate the horizontal (ordinary) and vertical (extraordinary) components of the optical constants, respectively.

Fig. 5(a) and (b) show the single crystal structures of 1,6 DAP-TP and DAC-TP. For 2,7 DAP-TP, a single crystal was not obtained. When looking at the single crystal results for 1,6 DAP-TP and DAC-TP, the twist angle (α) between anthracene and pyrene or chrysene was 78.4° and 74.5°, respectively, with a highly twisted core angle. The core-side angle (β) between anthracene and m-terphenyl group was 81.2° and 76.4°, respectively. Fig. 5(c-e) illustrate possible dimer stacking models of 1,6 DAP-TP, DAC-TP and 2,7 DAP-TP, computed using ωB97XD/6-31G(d) calculations.[23] In the calculated structures of dimer stacking, the angles of α and β were similar to those obtained experimentally for the single crystals (see Table S2). In the predicted structure of 2,7 DAP-TP, α and β values of 69.2° and 69.9° were identified. The similarity of the experimental and calculation results for 1,6 DAP-TP and DAC-TP indicates that the calculation results for 2,7 DAP-TP are likely to be valid. The three materials all showed highly twisted core structures, despite exhibiting excimer emission in the solid film state. The intermolecular anthracene-anthracene distance in the calculated dimer structures of 1,6 DAP-TP,

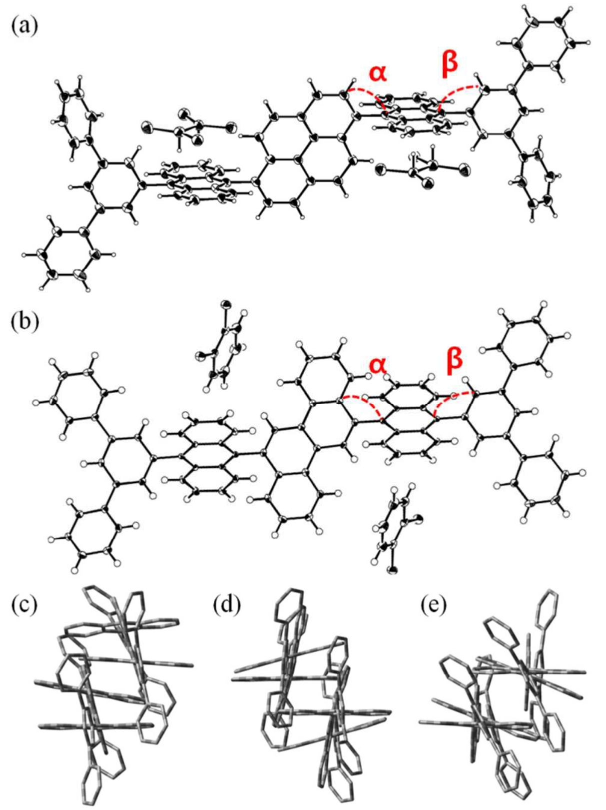

Fig. 5 The single crystal structures of (a) 1,6 DAP-TP·2(tetrachloroethane) and (b) DAC-TP·2(1,2-dichlorobenzene); and the dimer structures of (c) 1,6 DAP-TP, (d) DAC-TP, and (e) 2,7 DAP-TP, calculated using ωB97XD/6-31G(d).

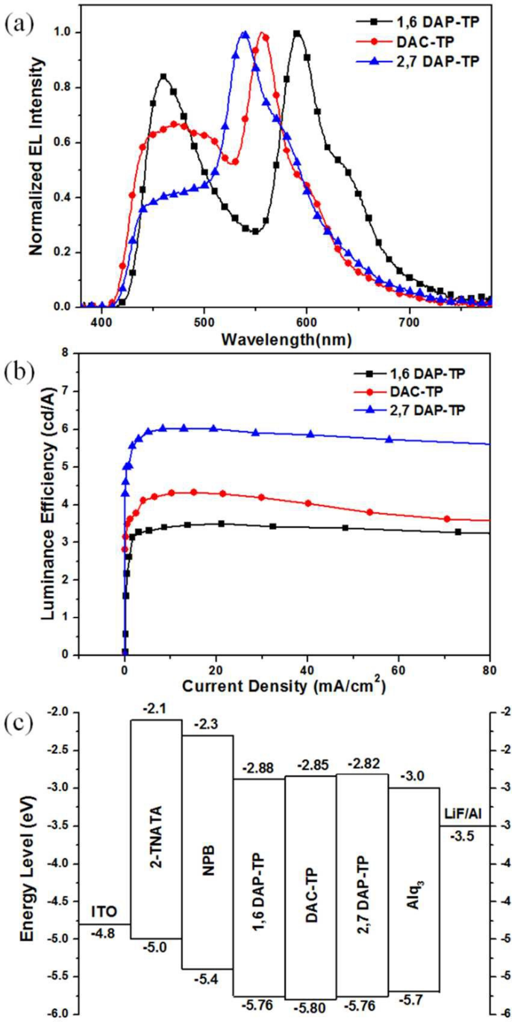

Fig. 6 EL characteristics of devices using the synthetic materials as EMLs: (a) EL spectra, (b) luminance efficiency versus current density, (c) energy diagrams of the compounds.

DAC-TP, and 2,7 DAP-TP was within the range of 3.5 Å to 3.8 Å, smaller than interplanar distance of 4.0 Å needed for effective intermolecular interaction.[24] This short intermolecular distance is thought to be the cause of anthracene–anthracene excimer formation. Based on the results from Mataga and Tian groups, excimer emission wavelength of anthracene is in the range of 460nm - 620nm according to the overlapped phenyl ring numbers between anthracenes.[15] It means that excimer wavelength can be modified by changing its molecular packing structure.[25] From this calculation, the overlap percentage of anthracene–anthracene in 1,6 DAP-TP, DAC-TP, and 2,7 DAP-TP was determined to be 67%, 60%, and 55%, respectively. The excimer emission values of 1,6 DAP-TP, DAC-TP, and 2,7 DAP-TP were 591 nm, 556 nm, and 537 nm, respectively. Therefore, the wavelength of excimer emission decreases as the overlap decreases. Thus, the excimer emission wavelength could be tuned by varying the center position in the triple-core chromophore derivatives.

The synthesized materials were used as non-doped emitting layers (EMLs) in OLEDs with the following structures: ITO/2-TNATA (60 nm)/NPB (15 nm)/synthesized material (35 nm)/Alq_3 (20 nm)/LiF (1 nm)/Al (200 nm). The OLED properties are summarized in Fig. 6, Fig. S5 and Table 2.

Fig. 6(a) shows the EL spectra of the fabricated devices. Excimer EL emission was observed at 591 nm for DAP-TP, 556 nm for DAC-TP, and 538 nm for 2,7 DAP-TP. The EL maximum

Table 2. EL performances: ITO/2-TNATA (60 nm)/NPB (15 nm)/the synthesized materials (35 nm)/Alq_3 (20 nm)/LiF (1 nm)/Al at 10 mA/cm^2

Compounds	V [a] (V)	LE [b] (Cd/A)	PE [c] (lm/W)	CIE (x,y) [d]	λ_{max} EL (nm)
1,6 DAP-TP	8.1	3.43	1.45	(0.37, 0.31)	460, 591
DAC-TP	8.5	4.30	1.76	(0.30, 0.37)	466, 556
2,7 DAP-TP	8.2	6.01	2.56	(0.32, 0.44)	464, 538

[a] Operating voltage. [b] Luminance efficiency. [c] Power efficiency . [d] Commission Internationale de l'Eclairage.

values of excimer emissions follow the same trend as the PL maximum values. The EL CIE coordinate values of 1,6 DAP-TP, DAC-TP, and 2,7 DAP-TP were (0.37, 0.31), (0.30, 0.37), and (0.32, 0.44), respectively, indicating white emission from all materials (see Fig. S6). Fig. 6(b) shows plots of luminance efficiency versus current density. Values of 3.43 cd/A, 4.30 cd/A, and 6.01 cd/A were measured at 10 mA/cm^2 for 1,6 DAP-TP, DAC-TP and 2,7 DAP-TP, respectively. The power efficiencies were 1.45 lm/W, 1.76 lm/W, and 2.56 lm/W, respectively. As a result, single molecular white emission was observed in the EL devices containing the synthesized compounds, and high device performance was identified through optimization of molecular structure and intermolecular interaction in the case of 2,7 DAP-TP.

Conclusions

Three triple-core chromophore derivatives based on anthracene and pyrene or chrysene moieties were synthesized and characterized. All three materials showed highly twisted core structures and exhibited excimer emission when prepared as a film. Excimer emission makes single molecular white emission possible, and can be interpreted by anisotropic intermolecular alignment (orientation effect). The maximum wavelength of excimer emission was controlled by varying the core chromophore at the center position of the triple-core chromophore, with excimer emission of 1,6 DAP-TP, DAC-TP, and 2,7 DAP-TP occurring at 591 nm, 556 nm, and 537 nm, respectively. When the three materials were used as an OLED emitting layer, the CIE coordinate values of 1,6 DAP-TP, DAC-TP, and 2,7 DAP-TP were (0.37, 0.31), (0.30,0.37), and (0.32, 0.44), respectively, indicating white emission. Especially, the device based on 2,7 DAP-TP acted as a WOLED with a high efficiency of 6.01 cd/A at 10 mA/cm^2. The present findings demonstrate that triple-core chromophores composed of various chromophores can be applied in OLED lighting applications.

Experimental

General information

The ^{1}H-NMR spectra and ^{13}C-NMR spectra were recorded on Bruker Avance 300 and Avance 500 spectrometers. The FAB$^+$-mass and EI$^+$-spectra were recorded on a JEOL, JMS-AX505WA, HP5890 series II. The optical absorption spectra were obtained by using a Lambda 1050 UV/Vis/NIR spectrometer (PerkinElmer). A PerkinElmer luminescence spectrometer LS50 (Xenon flash tube) was used to perform photoluminescence (PL) spectroscopy. The glass-transition temperatures (T_g) of the compounds were determined with differential scanning calorimetry (DSC) under a nitrogen atmosphere by using a DSC4000 (PerkinElmer). Degradation temperatures (T_d) were determined with thermogravimetric analysis (TGA) by using a TGA4000 (PerkinElmer).

Time-resolved fluorescence lifetime experiments were performed using the time-correlated single photon counting (TCSPC) technique implemented in a FluoTime200 spectrometer (PicoQuant) equipped with a PicoHarp300 TCSPC board (PicoQuant) and a PMA182 photomultiplier (PicoQuant). The excitation source was a 377 nm picosecond pulsed diode laser (PicoQuant, LDH375) driven by a PDL800-D driver (PicoQuant) with a FWHM of ~70 ps. The decay time fitting procedure was carried out using the IRF implemented in the Fluofit software (PicoQuant).

The HOMO energy levels were determined by ultraviolet photoelectron yield spectroscopy (Riken Keiki AC-2). The LUMO energy levels were derived from the HOMO energy levels and the band gaps. We determined the optimized structures and dimer structure using density functional theory (DFT) at the B3LYP/6-31G (d) and ωB97XD/6-31G (d) levels of theory, respectively.

The variable angle spectroscopic ellipsometry (VASE) measurements of the films prepared from the synthesized materials on Si substrates were performed using a fast spectroscopic ellipsometer (M-2000U, J. A. Woollam Co., Inc.) at seven angles of incident light ranging from 45° to 75° in steps of 5°. At each angle, the experimental ellipsometric parameters Ψ and Δ were simultaneously obtained in steps of 1.6 nm throughout the spectral region from 245 to 1000 nm. VASE data were analyzed using the WVASE32 (J. A. Woollam Co., Inc) software.

In each of the EL devices, tris(N-(naphthalen-2-yl)-N-phenyl-amino)triphenylamine (2-TNATA) was used for the hole injection layer (HIL), N,N'-bis(naphthalen-1-yl)-N,N'-bis(phenyl)benzidine (NPB) was used for the hole transporting layer (HTL), one of the synthetic materials 1,6 DAP-TP, DAC-TP and 2,7 DAP-TP was used as the emitting layer (EML), 8-hydroxyquinoline aluminum (Alq$_3$) was used for the electron transporting layer (ETL), lithium fluoride (LiF) was used for the electron injection layer (EIL), and ITO was used as the anode and Al as the cathode. All organic layers were deposited under 10^{-6} Torr, with a rate of deposition of 1 Å/s to create an emitting area of 4 mm^2. The LiF and aluminum layers were continuously deposited under the same vacuum conditions. The luminance efficiency data for the fabricated EL devices were obtained by using a Keithley 2400 electrometer. Light intensities were obtained with a Minolta CS-1000A.

Single crystal X-ray diffraction data of compound DAC-TP:

Single crystals suitable for X-ray analysis were obtained a o-dichlorobenzene solution of DAC-TP. Intensity data were collected at 100 K on a Bruker Single Crystal CCD X-ray Diffractometer (SMART APEX II ULTRA) with Mo Kα radiation (λ = 0.71073 Å) and graphite monochromator. A total of 16064 reflections were measured with a maximum 2 θ angle of 51.0˚, of which 5876 were independent reflections (R_{int} = 0.0564). The structure was solved by direct methods (SHELXS-97[26]) and refined by the full-matrix least-squares on F^2 (SHELXL-97[26]). All non-hydrogen atoms were refined anisotropically. All hydrogen atoms were placed using AFIX instructions. The crystal data are as follows: $C_{94}H_{60}Cl_4$ ($C_{82}H_{52}$ and $(C_6H_4Cl_2)_2$); FW = 1331.22, crystal size 0.13 × 0.08 × 0.08 mm^3, Monoclinic, $P2_1/c$, a = 9.6963(13) Å, b = 32.629(4) Å, c = 11.4490(16) Å, β =

113.025(2)°, V = 3333.6(8) Å^3, Z = 2, D_c = 1.326 g cm^{-3}. The refinement converged to R_1 = 0.0467, wR_2 = 0.1049 ($I > 2\sigma(I)$), GOF = 1.047.

Synthesis

1,6 DAP-TP and 4,4,5,5-tetramethyl-2-[1,1';3',1'']terphenyl-5'-yl-[1,3,2]dioxaborolane (compound 6) were obtained according to the procedures reported elsewhere.[19, 1g] ^{13}C NMR data could not be obtained because of the very low solubility of the DAC-TP.

Compound 2. Compound 1 (15.0 g, 58.3 mmol) was dissolved in anhydrous THF solution (200 ml) and stirred at -78 °C. Then, 2.0 M n-BuLi (35.0 mL, 70.0 mmol) was added. Triethyl borate (13.9 ml) was added to the reaction after 30 min. After the reaction had finished, the solution was acidified with 2 N HCl solution at room temperature and extracted with ethyl acetate and water. The organic layer was dried with anhydrous $MgSO_4$ and filtered. The solution was evaporated. The residue was re-dissolved in ethyl acetate and hexane was added into the solution. The precipitate was filtered and washed with hexane to obtain a beige compound (11.68 g, 90 %). ^{1}H-NMR (300 MHz, $CDCl_3$): δ= 8.47 (s, 1H), 8.14 (d, 2H), 8.04 (d, 2H), 7.53-7.44 (m, 4H), 5.07 (s, 2H), EI$^+$-Mass: 222.

Compound 4. Compound 2 (1.35 g, 6.08 mmol), compound 3 (0.90 g, 2.33 mmol), and $Pd(PPh_3)_4$ (0.539 g, 0.47 mmol) were added to a 100 ml / 10 ml anhydrous toluene / THF solution. Then, 2 M K_2CO_3 solution (30 ml) dissolved in H_2O was added to the reaction mixture at 50 °C. The mixture was refluxed for 5 h under nitrogen. After the reaction had finished, the mixture was filtered. The product was isolated using silica gel column chromatography with $CHCl_3$ as the solvent. The solvent was removed by evaporation. Recrystallization of the residue from $CHCl_3$ afforded a beige compound (0.78 g, 58 %). ^{1}H -NMR (300 MHz, [D_8]THF): δ= 9.07 (s, 2H), 8.99 (d, 2H), 8.75 (s, 2H), 8.21 (d, 4H), 7.63-7.55 (m, 6H), 7.52 (t, 4H), 7.33-7.24 (m, 8H), EI$^+$-Mass: 580.

Compound 5. Compound 4 (0.50 g, 0.86 mmol) and N-bromosuccinimide (NBS) (0.37 g, 2.07 mmol) were added to 200 mL $CHCl_3$, 200 ml CH_2Cl_2, and acetic acid (20 ml). The mixture was refluxed for 6 h. After the reaction had finished, the reaction mixture was extracted with $CHCl_3$ and water. The organic layer was dried with anhydrous $MgSO_4$ and filtered. The solution was evaporated. The residue was re-dissolved in $CHCl_3$ and added to ethanol. The precipitate was filtered and washed with acetone to obtain a yellow compound (0.52 g, 82 %). ^{1}H -NMR (300 MHz, [D_8]THF): δ= 9.08 (s, 2H), 8.99 (d, 2H), 8.73 (d, 4H), 7.69-7.62 (m, 8H), 7.60 (t, 2H), 7.38-7.31 (m, 6H), 7.24 (d, 2H), EI$^+$-Mass: 738.

DAC-TP. Compound 5 (0.50 g, 0.68 mmol), compound 6 (0.58 g, 1.63 mmol), $Pd(OAC)_2$ (0.056 g, 0.14 mmol), and $(cyclohexyl)_3P$ (0.057 g, 0.20 mmol) were added to a 240 ml / 60 ml anhydrous toluene / THF solution. Then tetraethylammonium hydroxide (20 wt%) (20.0 ml) was added to the reaction mixture at 50 °C. The mixture was refluxed for 3 h under nitrogen. After the reaction had finished, the mixture was filtered. The product was isolated using silica gel column chromatography with $CHCl_3$ as the solvent. The solvent was removed by evaporation. Recrystallization of the residue from $CHCl_3$ afforded a beige compound (0.35 g, 50 %). ^{1}H -NMR (300 MHz, [D_8]THF): δ= 9.16 (s, 2H), 9.05 (d, 2H), 8.22 (s, 2H), 8.00-7.96 (m, 6H), 7.92-7.86 (m, 10H), 7.73 (d, 4H), 7.67-7.61 (m, 2H), 7.53-7.47 (m, 8H), 7.44-7.38 (m, 12H), 7.33 (t, 4H); HRMS (EI, m/z): [M$^+$] calcd for C82H52, 1036.4147; found, 1036.4146. Anal. calcd for C82H52: C 94.95, H 5.05; found: C 94.84, H 5.06 %.

Compound 8. Compound 7 (4.0 g, 19.8 mmol), bis(pinacolato)diboron (11.1 g, 43.5 mmol), $[Ir(OMe)COD]_2$ (0.39 g, 0.59 mmol) and dmbpy (0.22 g, 1.19 mmol) were added to anhydrous THF (200 ml). The mixture was refluxed for 12 h under nitrogen. After the reaction had finished, the solution was extracted with ethyl acetate and water. The organic layer was dried with anhydrous $MgSO_4$ and filtered. The solution was evaporated. The product was isolated using silica gel column chromatography with CH_2Cl_2 as the solvent. The solvent was removed by evaporation. The residue was re-dissolved in $CHCl_3$ and MeOH was added into the solution. The precipitate was filtered and washed with MeOH to obtain a white compound (8.45 g, 94 %). ^{1}H-NMR (300 MHz, $CDCl_3$): δ= 8.61 (s, 4H), 8.08 (s, 4H), 1.46 (s, 24H), EI$^+$-Mass: 454.

Compound 9. Compound 8 (2.0 g, 4.40 mmol), compound 1 (2.26 g, 8.81 mmol), and $Pd(PPh_3)_4$ (1.02 g, 0.88 mmol) were added to a 100 ml / 10 ml anhydrous toluene / THF solution. Then, 2 M K_2CO_3 solution (30 ml) dissolved in H_2O was added to the reaction mixture at 50 °C. The mixture was refluxed for 5 h under nitrogen. After the reaction had finished, the mixture was filtered. The product was isolated using silica gel column chromatography with $CHCl_3$ as the solvent. The solvent was removed by evaporation. Recrystallization of the residue from $CHCl_3$ afforded a beige compound (0.68 g, 27.9 %). ^{1}H -NMR (300 MHz, [D_8]THF): δ= 8.67 (s, 2H), 8.38 (s, 4H), 8.27 (s, 4H), 8.17 (d, 4H), 7.65 (d, 4H), 7.51 (t, 4H), 7.35 (t, 4H), EI$^+$-Mass: 554.

Compound 10. Compound 9 (0.50 g, 0.90 mmol) and NBS (0.35 g, 1.98 mmol) were added to 300 ml $CHCl_3$, 100 mL CH_2Cl_2, and acetic acid (20 ml). The mixture was refluxed for 6 h. After the reaction had finished, the reaction mixture was extracted with $CHCl_3$ and water. The organic layer was dried with anhydrous $MgSO_4$ and filtered. The solution was evaporated. The residue was re-dissolved in $CHCl_3$ and added to ethanol. The precipitate was filtered and washed with acetone to obtain a yellow compound (0.53 g, 82 %). ^{1}H -NMR (300 MHz, [D_8]THF): δ= 8.70 (d, 4H), 8.39 (s, 4H), 8.30 (s, 4H), 7.69-7.64 (m, 8H), 7.42 (t, 4H), EI$^+$-Mass: 712.

2,7 DAP-TP. Compound 10 (0.40 g, 0.56 mmol), compound 6 (0.48 g, 1.34 mmol), $Pd(OAC)_2$ (0.046 g, 0.11 mmol), and $(cyclohexyl)_3P$ (0.047 g, 0.17 mmol) were added to a 240 ml /

20 ml anhydrous toluene / THF solution. Then tetraethylammonium hydroxide (20 wt%) (20.0 ml) was added to the reaction mixture at 50 °C. The mixture was refluxed for 3 h under nitrogen. After the reaction had finished, the mixture was filtered. The product was isolated using silica gel column chromatography with CHCl$_3$ as the solvent. The solvent was removed by evaporation. Recrystallization of the residue from CHCl$_3$ afforded a yellow compound (0.47 g, 83 %). ^{1}H -NMR (300 MHz, [D$_8$]THF): δ= 8.46 (s, 4H), 8.34 (s, 4H), 8.20 (s, 2H), 7.96 (d, 4H), 7.89-7.86 (m, 12H), 7.72 (d, 4H), 7.51-7.46 (m, 8H), 7.43-7.31 (m, 12H); ^{13}C-NMR (500 MHz, [D$_8$]THF): δ= 143.25, 141.89, 141.45, 138.39, 138.36, 132.77, 131.68, 131.19, 129.95, 129.84, 129.19, 129.15, 128.61, 128.28, 128.12, 127.99, 126.30, 125.93, 125.17; HRMS (EI, m/z): [M$^+$] calcd for C80H50, 1010.3991; found, 1010.3986. Anal. calcd for C80H50: C 95.02, H 4.98; found: C 94.88, H 5.07 %.

Acknowledgements

This research was supported by a grant from the Fundamental R&D Program for Core Technology of Materials funded by the Ministry of Trade, Industry and Energy, Republic of Korea (Project No. 10050215).

References

1 (a) C. W. Tang, S. A. Vanslyke, *Appl. Phys. Lett.*, 1987, **51**, 913; (b) J. Huang, X. Wang, A. J. deMello, J. C. deMello, D. D. C. Bradley, *J. Mater. Chem.,* 2007, **17**, 3551; (c) B. W. D'Andrade, S. R. Forrest, *Adv. Mater.,* 2004, **16**, 1585; (d) H. Uoyama, K. Goushi, K. Shizu, H. Nomura, C. Adachi, *Nature*, 2012, **492**, 234; (e) Z. Zhao, C. Deng, S. Chen, J. W. Y. Lam, W. Qin, P. Lu, Z. Wang, H. S. Kwok, Y. Ma, H. Qiu, B. Z. Tang, *Chem. Commun.,* 2011, **47**, 8847; (f) Y. I. Park, J. H. Son, J. S. Kang, S. K. Kim, J. H. Lee, J. W. Park, *Chem. Commun.*, 2008, 2143; (g) S. K. Kim, B. Yang, Y. Ma, J. H. Lee, J. W. Park, *J. Mater. Chem.*, 2008, **18**, 3376.

2 (a) C. D. Dimitrakopoulos, P. R. L. Malenfant, *Adv. Mater.*, 2002, **14**, 99; (b) A. R. Murphy, J. M. J. Fréchet, *Chem. Rev.*, 2007, **107**, 1066; (c) H. N. Tsao, D. M. Cho, I. Park, M. R. Hansen, A. Mavrinskiy, D. Y. Yoon, R. Graf, W. Pisula, H. W. Spiess, K. Müllen, *J. Am. Chem. Soc.*, 2011, **133**, 2605; (d) H. Chen, Y. Guo, G. Yu, Y. Zhao, J. Zhang, D. Gao, H. Liu, Y. Liu, *Adv. Mater.*, 2012, **24**, 4618; (e) F. Würthner, M. Stolte, *Chem. Commun.*, 2011, **47**, 5109; (f) Y. I. Park, J. S. Lee, B. J. Kim, B. J. Kim, J. H. Lee, D. H. Kim, S. Y. Oh, J. H. Cho, J. W. Park, *Chem. Mater.*, 2011, **23**, 4038; (g) H. E. Katz, Z. Bao, S. L. Gilat, *Acc. Chem. Res.*, 2001, **34**, 359.

3 (a) M. Reyes-Reyes, K. Kim, D. L. Carroll, *Appl. Phys. Lett.*, 2005, **87**, 083506; (b) S. H. Park, A. Roy, S. Beaupre, S. Cho, N. Coates, J. S. Moon, D. Moses, M. Leclerc, K. Lee, A. J. Heeger, *Nat. Photonics*, 2009, **3**, 297; (c) C. W. Schlenker, M. E. Thompson, *Chem. Commun.*, 2011, **47**, 3702; (d) G. Dennler, M. C. Scharber, C. J. Brabec, *Adv. Mater.*, 2009, **21**, 1323.

4 (a) B. K. An, J. Gierschner, and S. Y. Park, *Acc. Chem. Res.* 2012, **45**, 544; (b) C. Reese, M. E. Roberts, S. R. Parkin, and Z. Bao, *Adv. Mater.,* 2009, **21**, 3678; (c) H. C. Su, F. C. Fang, T. Y. Hwu, H. H. Hsieh, H. F. Chen, G. H. Lee, S. M. Peng, K. T. Wong, and C. C. Wu, *Adv. Funct. Mater.*, 2007, **17**, 1019; (d) J. Kalinowski, G. Giro, M. Cocchi, V. Fattori, and P. Di Marco, *Appl. Phys. Lett.*, 2000, **76**, 2352; (e) Z. G. Soos, S. Mukhopadhyay, S. Ramasesha, *Chem. Phys. Lett.*, 2007, **442**, 285; (f) S. Mukhopadhyay, B. J. Topham, Z. G. Soos, S. Ramasesha, *J. Phys. Chem. A*, 2008, **112**, 7271; (g) T. Seko, K. Ogura, Y. Kawakami, H. Sugino, H. Toyotama, J. Tanaka, *Chem. Phys. Lett.*, 1998, **291**, 438.

5 D. H. Kim, D. Y. Lee, H. S. Lee, W. H. Lee, Y. H. Kim, J. I. Han, Kilwon Cho, *Adv. Mater.*, 2007, **19**, 678.

6 J. Y. Hu, Y. J. Pu, Y. Yamashita, F. Satoh, S. Kawata, H. Katagiri, H. Sasabe, J. Kido, *J. Mater. Chem. C*, 2013, **1**, 3871.

7 S. Roy, S. P. Mondal, S. K. Ray, K. Biradha, *Angew. Chem. Int. Ed.,* 2012, **51**, 12012.

8 S. Tsuzuki, K. Honda, T. Uchimaru, M. Mikami, K. Tanabe, *J. Am Chem. Soc.*, 2002, **124**, 104.

9 T. Forster, K. Z. Kasper, *Phys. Chem. NF.*, 1954, **1**, 275.

10 (a) J. B. Birks, *Rep. Prog. Phys.*, 1975, **38**, 903; (b) H. Saigusa, E. C. Lim, *Acc. Chem. Res.*, 1996, **29**, 171.

11 P. P. Neelakandan , D. Ramaiah, *Angew. Chem. Int. Ed.*, 2008, **47**, 8407.

12 D. Mansell, N. Rattray, L. L. Etchells, C. H. Schwalbe, A. J. Blake, E. V. Bichenkova, R. A. Bryce, C. J. Barker, A. Diaz, C. Kremerf, S. Freeman, *Chem. Commun.*, 2008, 5161.

13 D. Thirion, M. Romain, J. R. Berthelot, C. Poriel, *J. Mater. Chem.*, 2012, **22**, 7149.

14 (a) G. Klaerner, M. H. Davey, W. D. Chen, J. C. Scott, R. D. Miller, *Adv. Mater.*, 1998, **10**, 993; (b) P. I. Shih, C. Y. Chuang, C. H. Chien, E. W. G. Diau, C. F. Shu, *Adv. Funct. Mater.*, 2007, **17**, 3141.

15 (a) T. Hayashi, N. Mataga, Y. Sakata, S. Misumi, M. Morita, J. Tanaka, *J. Am. Chem. Soc.*, 1976, **98**, 5910; (b) Y. Dong, B. Xu, J. Zhang, X. Tan, L. Wang, J. Chen, H. Lv, S. Wen, B. Li, L. Ye, B. Zou, W. Tian, *Angew. Chem. Int. Ed.*, 2012, **51**, 10782.

16 D. Yokoyama, *J. Mater. Chem.*, 2011, **21**, 19187.

17 (a) R. Häner, S. M. Biner, S. M. Langenegger, T. Meng, and V. L. Malinovskii, *Angew. Chem. Int. Ed.*, 2010, **49**, 1227; (b) X. Ni, S. Wang, X. Zeng, Z. Tao, and T. Yamato, *Org. Lett.*, 2011, **13**, 552; (c) R. H. Templer, S. J. Castle, A. R. Curran, G. Rumbles and D. R. Klug, *Faraday Discuss.*, 1998, **111**, 41; (d) M. R. Pokhrel and S. H. Bossmann, *J. Phys. Chem. B*, 2000, **104**, 2215.

18 (a) J. Kalinowski, M. Cocchi, D. Virgili, V. Fattori, and J. A. G. Williams, *Adv. Mater.*, 2007, **19**, 4000; (b) Z. Zhao, B. Xu, Z. Yang, H. Wang, X. Wang, P. Lu, and W. Tian, *J. Phys. Chem. C*, 2008, **112**, 8511.

19 J. Lee, B. Kim, J. E. Kwon, J. Kim, D. Yokoyama, K. Suzuki, H. Nishimura, A. Wakamiya, S. Y. Park, J. Park, *Chem. Commun.*, 2014, **50**, 14145.

20 (a) Y. M. Kim, J. Bouffard, S. E. Kooi, T. M. Swager, *J. Am. Chem. Soc.*, 2005, **127**, 13726; (b) R. Horiguchi, N. Iwasaki, Y.Maruyama, *J. Phys. Chem.*, 1987, **91**, 5135.

21 (a) J. Huber, K. Müllen, J. Salbeck, H. Schenk, U. Scherf, T. Stehlin, R. Stern, *Acta Polymer.*, **1994**, 45, 244; (b) G. Zeng, W. Yu, S. Chua, and W. Huang, *Macromolecules*. 2002, **35**, 6907; (c) A. C. Sen and B. Chakrabarti, *J. Biol. Chem.*, 1990, **265**,14277.

22 (a) D. Yokoyama, A. Sakaguchi, M. Suzuki, C. Adachi, *Appl. Phys. Lett.*, 2008, **93**, 173302; (b) D. Yokoyama, A. Sakaguchi, M. Suzuki, C. Adachi, *Org. Electron.*, 2009, **10**, 127; (c) D. Yokoyama, Y. Setoguchi, A. Sakaguchi, M. Suzuki, C. Adachi, *Adv. Funct. Mater.*, 2010, **20**, 386; (d) D. Yokoyama, H. Sasabe, Y. Furukawa, C. Adachi, J. Kido, *Adv. Funct. Mater*. 2011, **21**, 1375.

23 J. Aragó, J. C. Sancho-García, E. Ortí, D. Beljonne, *J. Chem. Theory Comput.*, 2011, **7**, 2068.

24 (a) E. A. Meyer, R. K. Castellano, F. Diederich, *Angew. Chem. Int. Ed.*, 2003, **42**, 1210; (b) Y. Dong, B. Xu, J. Zhang, X. Tan, L. Wang, J. Chen, H. Lv, S. Wen, B. Li, L. Ye, B. Zou, W. Tian, *Angew. Chem. Int. Ed.*, 2012, **51**, 10782.

25 (a) R. Akatsuka, A. Momotake, Y. Shinohara, Y. Kanna, T. Sato, M. Moriyama, K. Takahashi, Y. Nishimura, T. Arai, *J. Photoch. Photobio. A*, 2011, **223**, 1; (b) Z. Lin, S. Priyadarshy, A. Bartko,

D. H. Waldeck, *J. Photoch. Photobio. A*, 1997, **110**, 131; (c) S. Dey, P. Mondal and S. P. Rath, *New J. Chem.*, 2015, **39**, 4100.

26 Sheldrick, G. M. SHELX-97, Program for the Refinement of Crystal Structures; University of Göttingen: Göttingen, Germany, 1997.